

文章编号:1001-9014(2004)06-0401-04

FINITE DIFFERENCE TIME DOMAIN MODELING OF GRATING-COUPLED QUANTUM WELL INFRARED PHOTODETECTOR

SHU Xiao-Zhou, WU Yan-Rui, CHEN Xiao-Shuang, CHU Jun-Hao

(National Laboratory for Infrared Physics, Shanghai Institute of Technical Physics,
Chinese Academy of Sciences, Shanghai 200083, China)

Abstract: Diffraction grating is indispensable for quantum well infrared photodetectors (QWIP) in order to improve optical coupling because of the limitation of quantum selection rules. A numerical approach based on finite difference time domain (FDTD) method was presented for investigating the diffraction effect of a metal grating fabricated in QWIP. Simulation results demonstrate that such a complicated structure can be optimized by electromagnetic analysis based on the FDTD method. Detailed field distribution inside QWIP can be obtained for estimating the optical coupling efficiency of the grating.

Key words: quantum well infrared photodetector (QWIP); finite difference time domain (FDTD); diffracting grating

CLC number: 7820P **Document code:** A

时域有限差分法模拟量子阱红外探测器光栅的光耦合

疏小舟, 吴砚瑞, 陈效双, 褚君浩

(中国科学院上海技术物理研究所 红外物理国家重点实验室, 上海 200083)

摘要: 由于量子选择定则的限制, 对于量子阱红外探测器 (QWIP), 必须利用衍射光栅增强其光学耦合效率. 本文给出了一种基于时域有限差分法 (FDTD) 的数值方法, 计算制备在 QWIP 器件上的金属光栅的衍射效应. 模拟计算的结果表明, FDTD 方法是解析这种复杂结构内电磁场问题的有效手段. 可以计算 QWIP 器件内各点电磁场所有分量的详细分布, 进而可以估算衍射光栅的耦合效率, 以及优化 QWIP 结构设计.

关键词: 量子阱红外探测器 (QWIP); 时域有限差分法 (FDTD); 衍射光栅

Introduction

During the past decade, the quantum well infrared photodetectors (QWIP) have attracted much research attention for their advantage, i. e. high speed and very long wavelength availability^[1], in large focal plane array (FPA). However, quantum selection rules only allow the detection of the incident light with electric field component perpendicular to the quantum well planes. That means that the electric field of the incident light which is always parallel to the quantum well planes cannot be absorbed by the quantum well. One solution

is to fabricate a grating above the quantum well plane, so that some of the incident light propagates at some angles other than the perpendicular direction and becomes absorbable for QWIP^[1-3,4]. In this way, the grating improves the optical coupling between the incident light and QWIP. One typical grating is a periodically arranged metal patches or holes in the same dimension of wavelength^[5]. Obviously the optical coupling efficiency depends on the wavelength of incident light, the grating structure and its position. Some authors have studied the topic as a scalar diffraction process with Huygen's principle^[1,5]. The light intensi-

Received date: 2004 - 01 - 20, revised date: 2004 - 08 - 27

收稿日期: 2004 - 01 - 20, 修回日期: 2004 - 08 - 27

Foundation item: The project supported by "973" State Key Basic Research Program of China (2001CB610407)

Biography: SHU Xiao-Zhou (1968-), male, Anhui Chuzhou, doctor of physics, Research area is condensed matter physics.

ty absorbed by the QWIP is then estimated with the wave vector parallel to the quantum well plane. Strictly it is not the exact case that the quantum selection rules require, and the boundary condition at the grating interface has to be greatly simplified. In this paper, a numerical approach based on FDTD is developed to simulate diffraction effect of metal grating on QWIP. The only obstruction of its application is the high requirement on computer resources. How to decrease the requirement is an important research topic for FDTD^[7]. As regard to QWIP with metal grating, it is found that periodical boundary conditions are applicable to decrease the computational requirement greatly. A typical QWIP element is calculated as an example. All components of electromagnetic field are accurately obtained at any position inside the QWIP, which is used for investigating the diffraction effect of the metal grating.

1 Methodology

For numerical solution of Maxwell's equations, one main difficulty is the coupling between electric and magnetic fields, which is expressed as:

$$\nabla \times \mathbf{E} = -\mu \frac{\partial \mathbf{H}}{\partial t} \quad \nabla \times \mathbf{H} = \sigma \mathbf{E} + \varepsilon \frac{\partial \mathbf{E}}{\partial t} \quad (1)$$

The novel solution in FDTD method is to discretize the interested region into Yee's cells^[6]. Within the rectangular cell, all the components of electromagnetic fields are positioned at different points so as to implement finite difference from of the coupled equations conveniently. At each time step, components of electric field are updated with corresponding components of magnetic field at previous time step, and vice versa. The iteration algorithm for Z component of electric field is given as:

$$E_z^{n+1}(i, j, k + \frac{1}{2}) = E_z^n(i, j, k + \frac{1}{2}) + \frac{\Delta t}{\varepsilon_{i,j,k} \Delta x} [H_y^{n+\frac{1}{2}}(i + \frac{1}{2}, j, k + \frac{1}{2}) - H_y^{n+\frac{1}{2}}(i - \frac{1}{2}, k + \frac{1}{2})] + \frac{\Delta t}{\varepsilon_{i,j,k} \Delta y} [H_x^{n+\frac{1}{2}}(i, j - \frac{1}{2}) - H_x^{n+\frac{1}{2}}(i, j + \frac{1}{2}, k + \frac{1}{2})], \quad (2)$$

where i, j, k denote the numbers of Yee's cell, n is index of time step, $\Delta x, \Delta y$ and Δz describe the size of three dimensional cell, Δt is time step, and $\varepsilon_{i,j,k}$ is electric permittivity at the cell. Algorithm for other components of electromagnetic field has a similar form.

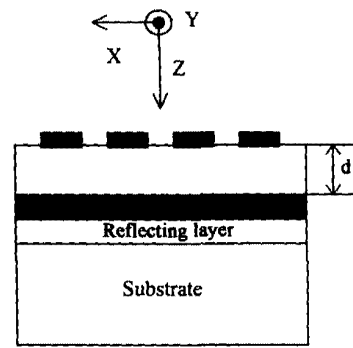


Fig. 1 Schematic structure of QWIP with diffraction grating
图1 具有衍射光栅的红外量子阱探测器结构图

Yee's cell size must be of tenths of an incident wavelength in order to avoid numerical inaccuracy. The time step must be kept small enough to prevent from dispersion in time iteration. The critical value can be estimated from cell size and light speed as:

$$\Delta t = \frac{1}{c \sqrt{\frac{1}{\Delta x^2} + \frac{1}{\Delta y^2} + \frac{1}{\Delta z^2}}} \quad (3)$$

In the computation, Mur's absorption boundary condition is employed^[8]. For normal incident wave, the first order Mur's absorption boundary condition can give high accuracy, and the reflectance is zero. But the reflectance will be about 0.17 if the incident angle is 45°. The first order Mur's absorption boundary condition(ABC) is applied only at the edges of the region. For non-edge points at ABC boundary, Mur's second order ABC is enforced. It is much more complicated in mathematics than the first order one. The reflectance will be about 0.03 in the case of the incident angle as 45°. While the region contains ideal conductor, special boundary condition must be enforced. All electromagnetic field components disappear inside ideal conductor. At interface between ideal conductivity and dielectric, the electric field is always perpendicular to the surface of the ideal conductor, and magnetic field parallel to it.

2 Numerical experiment

A typical structure of QWIP with metal grating is depicted in Fig. 1. The QWIP consists of multiple quantum wells and a two-dimensional grating above it. The grating is actually a pattern of periodically ar-

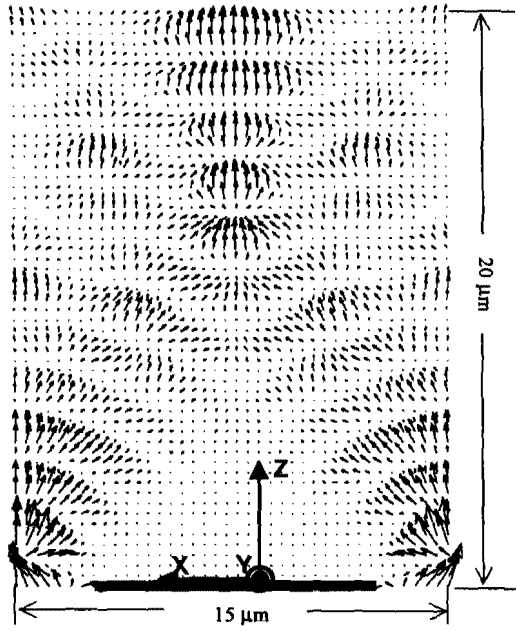


Fig. 2 Poynting vector distribution at one moment ($Y = 6\mu\text{m}$)

图2 某一时刻 Poynting 矢量分布图 ($Y = 6\mu\text{m}$)

ranged metal patches, in shape of circular, rectangular etc. Between the quantum well plane and the grating there is a spacing layer. A reflection layer is inserted between the quantum well and the substrate to improve the light absorption. To mesh the region, the size of Yee's cell must be small enough to describe the structural details of the QWIP and far smaller than the wavelength. Special attention should be paid to the dielectric layer, in which the large relative electric permittivity leads to a decreased wavelength. Generally the grating may consist of hundreds of metal patches or more.

If one simulates the QWIP as a whole, the task may lead to unacceptable requirement on computer memory and computing time. In fact, only the region corresponding to one metal patch is needed to compute with FDTD because of the translation invariance. The periodical boundary condition (PBC) is enforced at boundaries adjacent to other patches. At other boundaries, Mur's absorption boundary conditions are enforced.

During the simulation, incident plane wave is stimulated by electric dipoles at a plane before the grating. The electric dipoles oscillate with a certain frequency corresponding to destined light wavelength. The

incident light can be linearly polarized along any direction in X-Y plane. By the principle of superposition, it is then very convenient to investigate the non-polarized case.

The metal patches of the grating are set as rectangular shape, with $a = 10\mu\text{m}$, $b = 15\mu\text{m}$, and thickness as $0.5\mu\text{m}$. Wavelength of incident light is chosen as $10\mu\text{m}$ (in air), which is Y-polarized and propagates along Z direction. The relative electric permittivity of the spacing layer under the grating is assumed as 8.0. The size of Yee's cell is $0.125\mu\text{m} \times 0.125\mu\text{m} \times 0.125\mu\text{m}$. The total cell number is about 2.6million. Time step is set as 170ps. The simulation lasts 15000 steps.

A simple method to observe the diffraction effect of the grating is to calculate Poynting vector \mathbf{P} . At every time step, all optical field components within the computing region have been calculated with FDTD simulation. Therefore Poynting vector can be evaluated from them as:

$$\begin{bmatrix} P_x \\ P_y \\ P_z \end{bmatrix} = \begin{bmatrix} E_y H_z - E_z H_y \\ E_z H_x - E_x H_z \\ E_x H_y - E_y H_x \end{bmatrix} \quad (4)$$

Fig. 2 shows the distribution of magnitude of Poynting vector in the plane $Y = 6\mu\text{m}$, which is close to the center of metal patch. Obviously, Poynting vector is not aligned with Z axis everywhere because of the diffraction of metal grating. For the component of Poynting vector perpendicular to Z axis, the electric field may be in X, Y or Z directions. Only those in Z directions can be absorbed by QWIP, which can be written as:

$$\mathbf{P} = [-E_z H_x, E_z H_y, 0]^T \quad (5)$$

Being obtained in time domain, the field components within the simulated region oscillate harmonically. It is very difficult to evaluate optical coupling efficiency from Poynting vector distribution. Alternatively it may be more reasonable to derive it from energy density. The optical coupling efficiency at any Z plane can be given as:

$$\xi = \frac{\iint E_z(x, y, z)^2 dx dy}{\iint E_m(x, y, z_0)^2 dx dy} \quad (6)$$

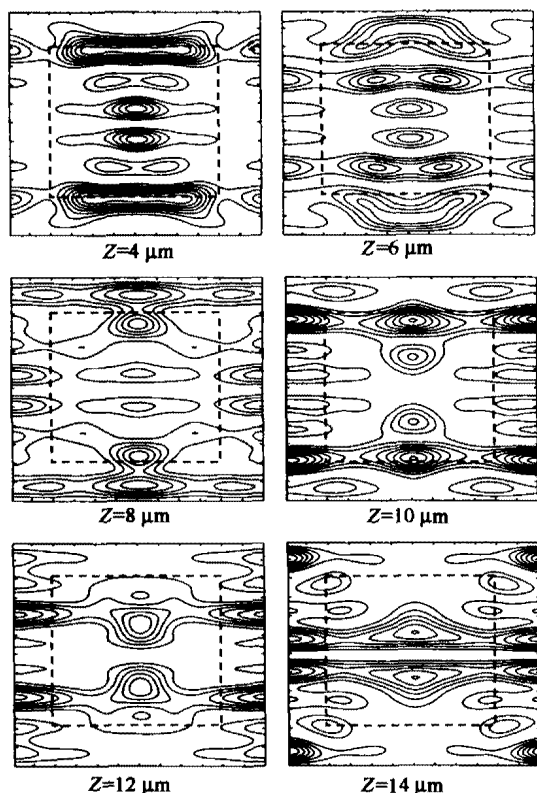


Fig. 3 Diffraction pattern for energy density from Z-component of electric field at different Z plane

图3 不同Z平面上电场Z分量的能量密度衍射图

While incident light is set as plane wave, z_0 in Eq. (6) can be any position between the electric dipoles and diffraction grating. The optical coupling efficiency is calculated to be about 0.005, being kept nearly the same value at different Z planes. Undoubtedly the coupling efficiency is strongly related with the wavelength of incident light, the shape and dimension of the metal grating etc. Different from coupling efficiency, the distribution of absorbable energy density varies with distance along Z direction rapidly. This can be observed from the diffraction pattern at different Z planes. Because of only the Z component of electric field being interested, the diffraction patterns shown in Fig. 3 are calculated by excluding X and Y components of electric field. The diffraction patterns are very help-

ful for determining the thickness of the spacing layer between the grating and the quantum plane.

3 Conclusion

By enforcing suitable boundary conditions, FDTD simulation can simulate detailed optical field distribution inside QWIP. Especially the distribution of electric field perpendicular with quantum plane, which is the only absorbable part for QWIP, can be directly obtained. As a numerical method, FDTD simulation can be applied without any limitation on the QWIP structure. The advantage makes FDTD method as a powerful tool for optimizing the grating structure to get high optical coupling efficiency.

REFERENCES

- [1] Fu Y, Willander M, Lu W, *et al.* Optical coupling in quantum well infrared photodetector by diffraction grating [J]. *J. Appl. Phys.*, 1998, **84**(10): 5750—5755.
- [2] Andersson J Y, Lundqvist L. Grating-coupled quantum-well infrared detectors: Theory and performance [J]. *J. Appl. Phys.*, 1992, **71**(7): 3600—3610.
- [3] Pan D, Li J M, Y P Zheng. *et al.* Long period two-dimensional gratings for 8-12 μ m quantum well infrared photodetectors [J]. *J. Appl. Phys.*, 1996, **80**(12): 7169—7171.
- [4] Goossen K W, Lyon S A, Alavi. Grating enhancement of quantum well detector response [J]. *Appl. Phys. Lett.*, 1998, **53**(12): 1027—1029.
- [5] Fu Y, Willander M, Li Ning. *et al.* Quantum mechanical model and simulation of GaAs/AlGaAs quantum well infrared photodetector-I optical aspects [J]. *J. Infrared Millim. Waves*, 2002, **21**(5): 187—192.
- [6] Yee K S. Numerical solution of initial boundary value problems involving Maxwell's equations in isotropic media [J]. *IEEE Trans. Antennas Propagat.*, 1966, **14**(3): 302—307.
- [7] Kondylis G D, Flaviis F D, Pottie G J. *et al.* A memory-efficient formulation of the finite-difference time domain method for the solution of Maxwell equations [J]. *IEEE Trans. on Microwave Theory and Tech.*, 2001, **49**(7): 1310—1320.
- [8] Mur G. Absorbing boundary conditions for the finite difference approximation of time domain electromagnetic field equations simulation of waves [J]. *IEEE Transactions on Magnetic Computability*, 1981, **23**(4): 377—382.